

CO₂ FORMATION IN QUIESCENT CLOUDS: AN EXPERIMENTAL STUDY OF THE CO + OH PATHWAY

J. A. NOBLE^{1,2}, F. DULIEU², E. CONGIU², AND H. J. FRASER¹

¹ Department of Physics, Scottish Universities Physics Alliance, University of Strathclyde, Glasgow, G4 ONG, UK

² LERMA-LAMAP, Université de Cergy-Pontoise, Observatoire de Paris, ENS, UPMC, UMR 8112 du CNRS, 5 mail Gay Lussac, 95000 Cergy Pontoise Cedex, France; francois.dulieu@obspm.fr

Received 2011 February 1; accepted 2011 March 29; published 2011 June 24

ABSTRACT

The formation of CO₂ in quiescent regions of molecular clouds is not yet fully understood, despite CO₂ having an abundance of around 10%–34% H₂O. We present a study of the formation of CO₂ via the nonenergetic route CO + OH on nonporous H₂O and amorphous silicate surfaces. Our results are in the form of temperature-programmed desorption spectra of CO₂ produced via two experimental routes: O₂ + CO + H and O₃ + CO + H. The maximum yield of CO₂ is around 8% with respect to the starting quantity of CO, suggesting a barrier to CO + OH. The rate of reaction, based on modeling results, is 24 times slower than O₂ + H. Our model suggests that competition between CO₂ formation via CO + OH and other surface reactions of OH is a key factor in the low yields of CO₂ obtained experimentally, with relative reaction rates of $k_{\text{CO+H}} \ll k_{\text{CO+OH}} < k_{\text{H}_2\text{O}_2+\text{H}} < k_{\text{OH+H}}, k_{\text{O}_2+\text{H}}$. Astrophysically, the presence of CO₂ in low A_V regions of molecular clouds could be explained by the reaction CO + OH occurring concurrently with the formation of H₂O via the route OH + H.

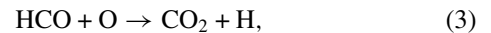
Key words: astrochemistry – ISM: molecules – methods: laboratory

1. INTRODUCTION

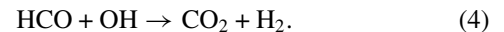
The first observations of solid CO₂ (henceforth CO_{2(s)}) were made by the *Infrared Astronomical Satellite (IRAS)*; D’Hendecourt & Jourdain de Muizon 1989). The molecule has since been observed in numerous environments, including toward galactic center sources (de Graauw et al. 1996), massive protostars (Gerakines et al. 1999; Gibb et al. 2004), low-mass young stellar objects (Nummelin et al. 2001; Pontoppidan et al. 2008), background stars (Knez et al. 2005), and in other galaxies (Shimonishi et al. 2010; Oliveira et al. 2011). Based on these observations, CO_{2(s)} is seemingly ubiquitous, and one of the most abundant solid-phase molecular species, approximately 10%–34% H₂O. It is believed to form in the solid phase, due to low gas-phase abundances (van Dishoeck et al. 1996), with evidence suggesting that much CO_{2(s)} production occurs in quiescent regions (Pontoppidan 2006; Nummelin et al. 2001); yet the key question remains: How does CO_{2(s)} form?

Many experimental studies have been performed to study the energetic formation routes to CO₂. Irradiation of pure CO ices with photons (Gerakines et al. 1996), charged particles (Palumbo et al. 1998), and electrons (Jamieson et al. 2006) have yielded CO₂. Similar experiments with mixtures of CO and H₂O were also successful (Ehrenfreund et al. 1997; Palumbo et al. 1998; Ioppolo et al. 2009; Laffon et al. 2010). The irradiation of hydrogenated carbon grains with ions and electrons produced small quantities of CO and CO₂ (Mennella et al. 2004, 2006).

CO_{2(s)} is abundant in quiescent as well as star-forming regions. While the role of energetic pathways cannot be discounted entirely in these regions (Whittet et al. 1998), the study of nonenergetic formation routes is fundamental to fully understanding the observed abundances of CO_{2(s)}. Potential nonenergetic formation routes (Ruffle & Herbst 2001) are



and



Theoretical studies of route (1) suggest that the formation of CO₂ proceeds with a high barrier of around 2500–3000 K, lowered on surfaces via the hot O atom or Eley–Rideal mechanisms (Talbi et al. 2006; Goumans et al. 2008). A solid-phase study determined that this pathway was feasible only via reaction in water pores, under a water ice cap, and upon heating (Roser et al. 2001), suggesting that it would not occur under the conditions present in quiescent molecular clouds. Reactions (3) and (4) have never been studied expressly in the solid phase.

Route (2) has been extensively studied in the gas phase, both experimentally (Frost et al. 1993; Fulle et al. 1996; Baulch et al. 2005) and theoretically (Yu et al. 2001; Chen & Marcus 2005; Sun & Law 2008), due to its importance in atmospheric and combustion chemistry. Recently, reaction (2) was experimentally studied in the solid phase by reflection–absorption infrared spectroscopy (RAIRS) for the first time, with positive results (Oba et al. 2010). Due to the limitations of the adopted method, it was not possible to produce a pure beam of OH, and therefore the chemistry is difficult to constrain with a simple series of reactions; in particular, it was experimentally complex to distinguish among reactions (2)–(4). OH was produced in the gas phase via a plasma discharge of H₂O, a process that yields a mixture of products including OH, H, H₂, O, and O₂. Although it is claimed that all OH radicals are in the rovibrational ground state due to collisions with the beam walls, well-defined spectroscopic studies of plasma discharges suggest that interaction with the walls is likely to lead to OH recombination, rather than yield ground-state OH, and that the major components of a plasma of H₂O are H₂ and H₂O, with lower abundances of OH (Médard et al. 2002; Fujii et al. 2002). Furthermore, experiments in the absence of CO produced H₂O₂ and O₃ whose yields varied with surface temperature, suggesting that surface temperature itself, mobility of the discharge products on the surface, and, potentially, the desorption rate of CO from the surface rather than

the rovibrational state of the OH is responsible for the changing yields of CO₂ observed at different temperatures. Finally, reaction (2) was found to proceed with little or no barrier, suggesting the presence of rovibrationally excited OH. We contend that, under these conditions, the CO₂ yield cannot be assumed to be independent of the excitation state of OH and thus further study of reaction (2) is imperative. A subsequent RAIRS study produced OH in the solid phase from a mixture of O₂:CO in a multilayer regime (Ioppolo et al. 2011b). Due to the multilayer regimes investigated, both previous studies also involved more complex chemistry than simply CO₂ formation, such as the formation of H₂CO₃ and CH₃OH, which further complicates the quantitative analysis of reaction (2).

Here, we present the first temperature-programmed desorption (TPD) spectra of CO_{2(s)} formed via reaction (2) in the solid phase, under interstellar conditions of temperature and pressure. In this study, OH was produced on the surface by the reaction of O₂ and O₃ with H in order to better constrain the reaction pathways in the system. The reaction was studied on both an amorphous silicate and a nonporous water surface, in a low-coverage regime, with the aim of limiting chemistry to only CO₂ production. In contrast to previous studies, a simple kinetic model was developed to determine relative reaction efficiencies and calculate the activation energy of reaction (2).

2. EXPERIMENTAL

Experiments were performed using the FORMOLISM apparatus (Amiaud et al. 2006). Briefly, the experimental setup consists of an ultrahigh-vacuum chamber (base pressure $\sim 10^{-10}$ mbar), containing an amorphous silicate-coated copper surface (5–400 K; Lemaire et al. 2010). Molecules are dosed onto the surface via two triply differentially pumped beam lines. Desorption of molecules from the surface is monitored using a quadrupole mass spectrometer (QMS) positioned directly in front of the surface. Experiments were performed on either bare silicate, or a nonporous, amorphous water film (*np*-H₂O) of ~ 100 monolayers (ML) grown on the silicate by spraying water vapor from a microchannel array doser (held at 120 K during water desorption, then cooled to 10 K before commencing the experiments).

Two different surfaces were investigated in order to (a) mimic two interstellar environments and (b) to determine the surface dependency of route (2). Amorphous silicate is an appropriate mimic of interstellar dust grains, composed of siliceous and carbonaceous material (Greenberg 2002). In molecular clouds these grains are covered in an ice mantle, the largest component of which is H₂O, at abundances of up to 100 ML (Williams & Herbst 2002). We used *np*-H₂O in this study to eliminate the complexity of chemistry occurring in pores.

Neither O₃ nor O₂ has been observed in an interstellar ice, so these experimental conditions are not directly astrophysically relevant but were used to produce OH in a controlled, reproducible manner. It is experimentally complex to create, maintain, and deposit onto a surface a pure, stable beam of the OH radical in the ground state. Thus, in this work, OH was produced on the surface via two routes: the hydrogenation of O₂ and that of O₃. O₂ is easier to utilize experimentally, but a study involving both species constrains reaction mechanisms better than using a single species. Due to the limits of sensitivity of the QMS, quantities below 0.1 ML were not investigated.

OH was not measured directly on the surface, due to its short lifetime, but the production of O₂, H₂O₂, and H₂O during control experiments on the hydrogenation of O₂ and O₃ confirms its

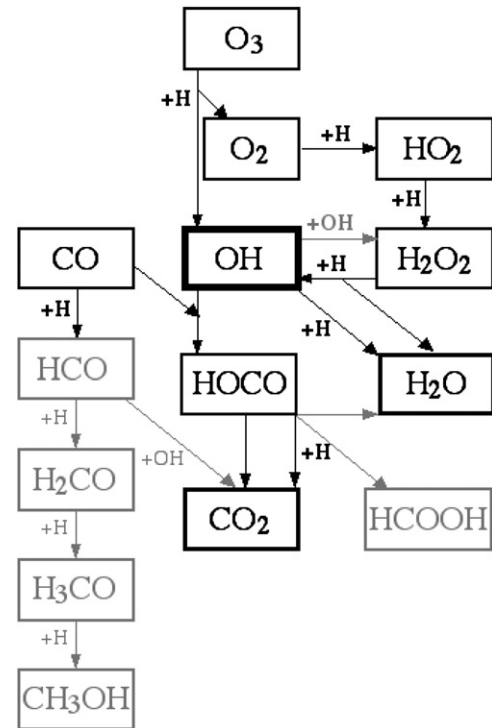


Figure 1. Chemical network of OH as a schematic diagram. Reactions which occurred in the present study are depicted in black, while those that did not are shaded gray. See the text for details.

Table 1
Experiments Performed in This Work

Experiment (Label)	Substrate	$N(\text{O}_2)$ (ML)	$N(\text{O}_3)$ (ML)	$N(^{13}\text{CO})$ (ML)	$t(\text{H})$ (minutes)
A	H ₂ O	0.5	...	0.6 [†]	0
B	H ₂ O	0.5	...	0.6 [†]	10
C	H ₂ O	0.5	...	0.6 [†]	20
D	H ₂ O	...	1.6	0.5	0
E	H ₂ O	...	1.4	0.5	2
F	H ₂ O	...	1.6	0.5	10
G	H ₂ O	...	1.1	0.6	20
H	Silicate	0.45	...	0.45	0
I	Silicate	0.45	...	0.45 [†]	20
J	Silicate	...	1.5	0.13	0
K	Silicate	...	1.3	0.45	20

Notes. Species were deposited on the surface in order from left to right, apart from those marked [†], where ¹³CO was deposited first. All species except ¹³CO were deposited using the same beam (see Section 2 for details).

presence, according to the reaction scheme:

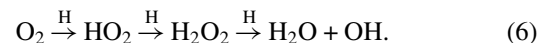


Figure 1 describes the chemical network of OH relevant to these experiments. The OH radical, produced by reactions (5) and (6), could react with CO as in reaction (2) to produce CO₂, or with H to form H₂O; thus, the relative rate of these reactions is an important factor determining the yield of CO₂ and the aim of this work was to elucidate the relative rates of these reactions.

All experiments are summarized in Table 1; approximately 1.5 ML of O₃ or 0.5 ML of O₂ were dosed onto the surface

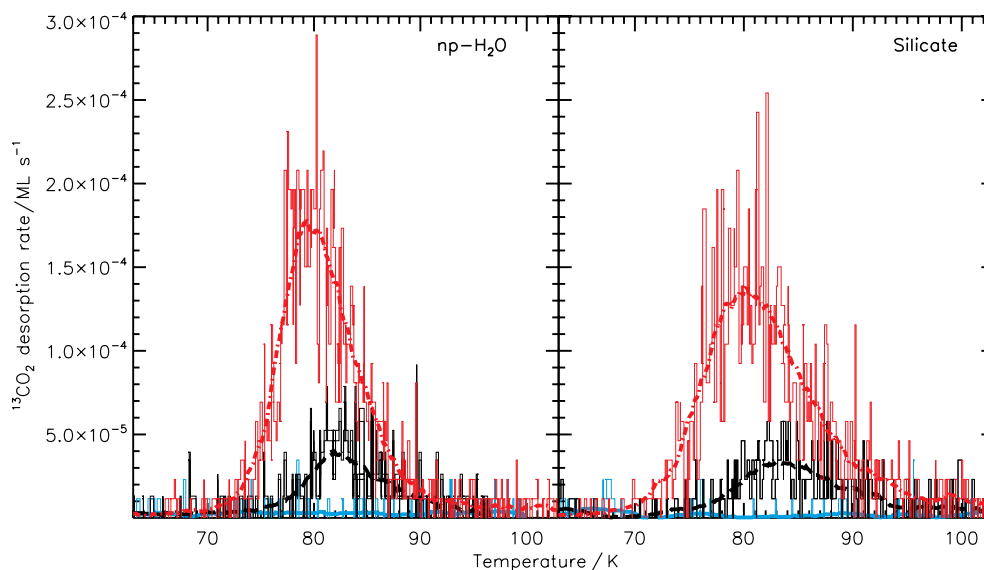


Figure 2. Temperature-programmed desorption spectra of Mass 45 ($^{13}\text{CO}_2$). The left panel shows desorption from a water surface, while the right panel shows a bare silicate surface. Experimental data are plotted in their raw form, accompanied by a smoothed version to guide the eye. Curves are labeled as follows: solid blue line, experiments A and H (0.5 ML O_2 , ~ 0.5 ML ^{13}CO , no H irradiation); dashed black line, experiments C and I (0.5 ML O_2 , ~ 0.5 ML ^{13}CO , 20 minutes H irradiation); dot-dashed red line, experiments G and K (~ 1 ML O_3 , ~ 0.5 ML ^{13}CO , 20 minutes H irradiation). Production of $^{13}\text{CO}_2$ is seen for both starting molecules (O_2 and O_3) on both surfaces, but O_3 yields significantly more $^{13}\text{CO}_2$ than O_2 . There is no discernible surface dependence of the reaction under current experimental conditions.

via one molecular beam, followed by ~ 0.5 ML of isotopically labeled ^{13}CO via a second beam. Finally, H atoms were deposited, via a plasma discharge of H_2 on beam 1, for a range of exposure times between 0 and 20 minutes. The deposition rate of H on the surface was $\sim 5 \times 10^{12}$ atoms $\text{cm}^{-2} \text{s}^{-1}$, taking into account the dosing pressure and the dissociation rate of H_2 (Amiaud et al. 2007). During O_3 deposition, the surface was held at 45 K to ensure that any traces of O_2 present in the O_3 beam desorbed from the surface (for detailed O_3 production method, see Mokrane et al. 2009); it was then cooled to 10 K before continuing. For all other molecules, the surface was held at 10 K during dosing.

H atoms were hot when produced in the plasma discharge of H_2 , but cooled to room temperature before exiting the molecular beam, due to collisions with the walls. Isotopically labeled ^{13}CO was used to avoid contamination of the results by $^{12}\text{CO}_2$ or ^{12}CO , pollutants present at very low gaseous concentrations in the chamber.

To measure the products of the reaction, the surface was heated from 10 to 100 K; desorbing molecular species were monitored with the QMS. Each TPD cycle lasted approximately three hours.

3. RESULTS AND DISCUSSION

Figure 2 shows TPD spectra of $^{13}\text{CO}_2$ produced by H irradiation of O_3 with ^{13}CO , and O_2 with ^{13}CO . $^{13}\text{CO}_2$ was produced during all experiments where H irradiation was performed. The $^{13}\text{CO}_2$ desorbs from each surface over a similar temperature range, but with a slightly different peak shape, indicative of the roughness of the underlying surfaces. It is clear that, since all data in Figure 2 are measured at the same H irradiation time, substantially more $^{13}\text{CO}_2$ is produced by the reaction of O_3 than that of O_2 . This is evident from reactions (5) and (6): three hydrogenation steps are required to generate a single OH radical from O_2 , whereas O_3 generates an OH radical directly.

As the solid blue line in Figure 2 shows, if the experiment was conducted without H irradiation, no $^{13}\text{CO}_2$ was produced. Nor was $^{13}\text{CO}_2$ production seen during control TPDs of ^{13}CO , O_2 , or O_3 . When ^{13}CO was not present, H_2O and H_2O_2 formed, rather than $^{13}\text{CO}_2$. It was assumed that all the $^{13}\text{CO}_2$ formed during H irradiation, in agreement with previous experiments (Oba et al. 2010; Ioppolo et al. 2011b). Within the limits of measurement, no gas-phase $^{13}\text{CO}_2$ was observed during the irradiation, indicating that the $^{13}\text{CO}_2$ remained on the surface. No additional $^{13}\text{CO}_2$ was produced during the TPDs because control experiments, where O_3 was irradiated with H before the deposition of ^{13}CO , yielded negligible $^{13}\text{CO}_2$, suggesting that when OH is produced it reacts quickly on the surface.

When searched for, we saw no evidence of the production of H^{13}COOH , validating the hypothesis that investigating a sub-monolayer coverage restricts the chemistry to CO_2 production, unlike previous studies (Oba et al. 2010; Ioppolo et al. 2011b). Nor were H^{13}CO or $^{13}\text{CH}_3\text{OH}$ seen in desorption. However, H_2 , ^{12}CO , ^{13}CO , and $^{12}\text{CO}_2$ were seen during all TPDs; $^{13}\text{CO}_2$ was seen upon H irradiation; H_2O_2 and H_2O were seen upon H irradiation, during extended TPDs to higher temperature; O_3 was seen only when O_3 had been deposited; and O_2 was seen in all experiments, except those with O_3 and no H irradiation.

Figure 3 illustrates $^{13}\text{CO}_2$ production as a function of H irradiation time (solid symbols). It is clear that $^{13}\text{CO}_2$ was produced at comparable rates on both surfaces (solid triangles versus solid squares), regardless of the starting material (O_2 or O_3), vindicating our earlier conclusion that the underlying surface does not play a significant role in this reaction. In every experiment, some ^{13}CO desorbed during the TPD, suggesting it was present in excess and never completely reacting with OH or H. In addition, O_3 , O_2 , and H were dosed via one beam while ^{13}CO was dosed via a second, and even after alignment the maximum overlap attainable is less than 100%, so not all reagents were dosed on the same region of the surface. However, as Figure 3 shows, the reactions are very sensitive to the quantity of OH generated, which itself depends upon

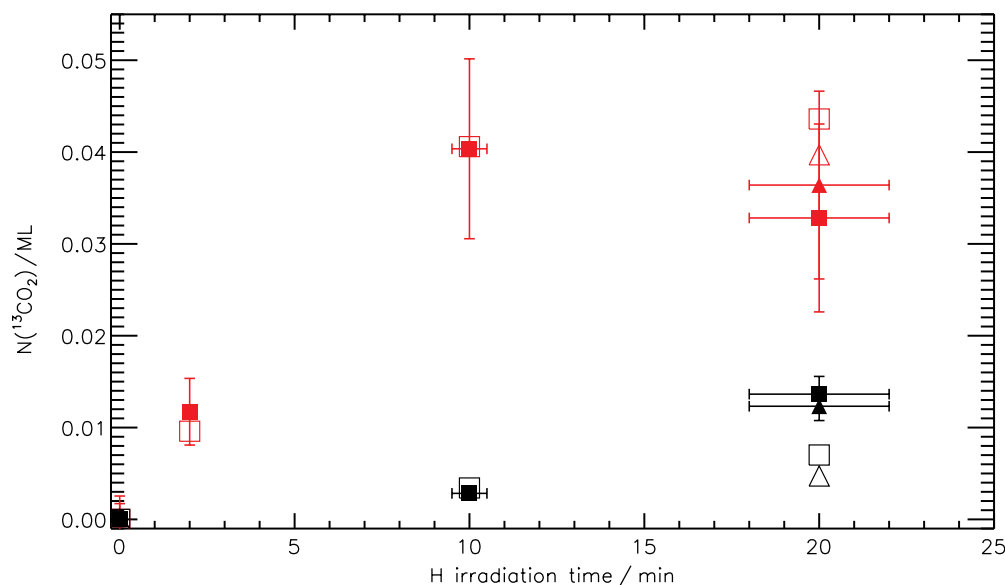


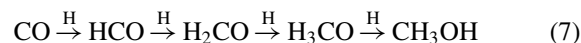
Figure 3. Evolution of $^{13}\text{CO}_2$ with H irradiation time, presented in ML of CO_2 , for all experiments. The data are labeled as follows: red closed squares, $\text{O}_3 + ^{13}\text{CO}$ on $np\text{-H}_2\text{O}$; red closed triangles, $\text{O}_3 + ^{13}\text{CO}$ on silicate; black closed squares, $\text{O}_2 + ^{13}\text{CO}$ on $np\text{-H}_2\text{O}$; black closed triangles, $\text{O}_2 + ^{13}\text{CO}$ on silicate. Overplotted (as corresponding open shapes) are the results of the kinetic model developed to describe the formation of $^{13}\text{CO}_2$. See the text for details.

the starting quantity of O_2 or O_3 on the surface. Although surface coverages were controlled to within ± 0.2 ML between experiments, this difference was sufficient to account for the varying concentration of $^{13}\text{CO}_2$ observed in Figure 3.

The maximum yield of $^{13}\text{CO}_2$ was $\sim 8\%$ with respect to ^{13}CO (Table 1, experiments F and K); the presence of a complex barrier helps to explain this. Gas phase and theoretical studies predict a three-stage barrier (~ 500 K; e.g., Frost et al. 1993; Yu et al. 2001). The reaction proceeds via an energetic HOCO intermediate, which isomerizes from *trans*-HOCO to *cis*-HOCO, before dissociating to form CO_2 (Smith & Zellner 1973; Alagia et al. 1993; Lester et al. 2000). Lester et al. (2001) suggest that a precursor OH-CO complex forms prior to the HOCO intermediate. On a surface, the reaction probability is even more reliant upon the relative orientation of CO and OH. A recent theoretical study on a coronene surface shows that OH physisorbs with the H atom pointing toward the surface (Goumans et al. 2008). Compared to the gas phase, the activation barrier to *trans*-HOCO formation is slightly lowered, and the intermediate is stabilized. A barrierless reaction between this stabilized HOCO complex with an additional H atom could produce $\text{CO}_2 + \text{H}_2$. However, experiments suggest this reaction could also yield HCOOH or $\text{H}_2\text{O} + \text{CO}$ (Ioppolo et al. 2011a), while reaction with OH could yield H_2CO_3 (Oba et al. 2010). From the results presented here, it is not possible to determine whether $^{13}\text{CO}_2$ formed from *cis*-HOCO $\rightarrow \text{CO}_2 + \text{H}$, or by hydrogenation of HOCO, although no H^{13}COOH was observed when TPDs were run to 200 K; thus we assume that, under our experimental conditions, reaction (2) produces only $^{13}\text{CO}_2$.

This complex barrier somewhat explains the low $^{13}\text{CO}_2$ yields, but there are further constraints to be considered. Due to the low coverages investigated here, the probability of ^{13}CO and OH meeting on the surface is small. OH recombination could produce H_2O_2 , or the competitive reaction $\text{OH} + \text{H}$ could remove OH from the surface (Ioppolo et al. 2008). Also, in these experiments, ^{13}CO was dosed after O_3 or O_2 , so at high enough coverages it could block H from reaching these reagents, allowing CO hydrogenation to artificially dominate. Previous studies show that hydrogenation of O_3 (Mokrane et al. 2009)

and O_2 (Ioppolo et al. 2008; Dulieu et al. 2010) occurs with no barrier, while hydrogenation of CO proceeds via



with a barrier of 390 K at 12 K to $\text{CO} + \text{H}$ (Fuchs et al. 2009; Watanabe & Kouchi 2002). Here, the ^{13}CO surface coverage was always below 1 ML, and neither H_2^{13}CO nor $^{13}\text{CH}_3\text{OH}$ desorbed during extended TPDs, indicating that little ^{13}CO hydrogenation occurred. If H^{13}CO was not produced in significant concentrations via reaction (7), it follows that $^{13}\text{CO}_2$ was not produced at measurable quantities via reaction (4), not least due to the low probability of any H^{13}CO produced encountering OH on the surface. These conclusions indicate that in this experiment $^{13}\text{CO}_2$ formation occurred exclusively via reaction (2).

A simple kinetic model of the experimental system was developed to describe the production of $^{13}\text{CO}_2$ via reaction (2), based on a set of coupled first-order rate equations. Figure 1 shows the potential detailed reaction scheme for these experiments. However, as illustrated above, given the low surface coverages employed here, a number of reactions, for example OH recombination, can be eliminated and are thus shown in gray in the figure. Neither CO_2 nor HCOOH reacts further with H (Bisschop et al. 2007), so such reactions were also ignored in the model. As discussed above, H^{13}CO was likely not produced at significant concentrations in these experiments. However, the rate of CO hydrogenation under present conditions was constrained by control experiments with only CO on the surface. It was assumed that the underlying surface had no effect on the reaction rate (as illustrated by Figure 3), so the model treats both surfaces simultaneously. The best fit to the experimental data was found by varying the rates of reaction, k_i , of $\text{CO} + \text{OH}$ and $\text{H}_2\text{O}_2 + \text{H}$, while constraining all other k_i with empirical data (reactions shown in black in Figure 1). That only two free parameters ($k_{\text{CO}+\text{OH}}$ and $k_{\text{H}_2\text{O}_2+\text{H}}$) were required to fit all of the data presented here provides strong evidence for the validity of the model and for the validity of our previous deductions that all $^{13}\text{CO}_2$ in our experiments was produced via reaction (2).

Table 2
Modeled Relative Rate Constants

Reaction	k_i/k_{O_2+H}
$O_3 + H$	1
$O_2 + H$	1
$HO_2 + H$	1
$H_2O_2 + H$	0.125 [†]
$CO + H$	0.025
$OH + H$	1
$CO + OH$	0.042 [†]

Notes. Rate was a free parameter in the model for reactions marked †. All other rates were fixed, based on published empirical values detailed in the text.

The results of the model are plotted over the experimental data as open symbols in Figure 3 and are summarized in Table 2. At low H irradiation times, the model describes well the production of $^{13}CO_2$, but starts to deviate slightly at longer times. This can be attributed to route (4) becoming competitive, but in that case, the O_3 and O_2 experiments should deviate with the same trend, while in reality the production of $^{13}CO_2$ from O_3 is slightly overestimated and that from O_2 is underestimated. Reaction (5) is exothermic (McKinley et al. 1955), so the excess energy of this reaction could be transferred to the products, which may then desorb from the surface. The model does not account for this possibility, and thus overestimates the $^{13}CO_2$ yield by the O_3 route.

The model, although a simplistic approach to explaining the surface chemistry because it ignores the complexity of the barrier known to exist in the $CO + OH$ pathway, suggests that the relatively low yield of $^{13}CO_2$ in these experiments results from competition between reaction (2) and other reactions involving OH. The relation between key reaction rates is

$$k_{CO+H} \ll k_{CO+OH} < k_{H_2O_2+H} < k_{OH+H}, k_{O_2+H}, \quad (8)$$

indicating that water formation should always dominate the formation of ice species at low surface coverages. The overall effective reaction rate of $CO + OH$ was determined to be 24 times slower than the hydrogenation of OH, O_3 , or O_2 , and 1.7 times faster than $CO + H$. The relative rate between the hydrogenation of O_2 and CO was 40, while between the hydrogenation of O_2 and H_2O_2 it was 8, consistent with literature values of 31–90 and 3.3, respectively (Miyachi et al. 2008). The factor-of-two difference between this and the previous value of $k_{O_2+H}/k_{H_2O_2+H}$ can be explained by the fact that molecular species such as H_2O_2 were more accessible to H in our (approximately 1 ML) experiments and therefore reacted more quickly than in the multilayer regime of Miyachi et al. (2008).

It is not possible to extract the activation barrier for HOCO formation or its subsequent reactions to form CO_2 in reaction (2) from the model. We can, however, calculate an effective barrier to CO_2 production by comparing our modeled relative rates to the activation barrier of 390 K at 12 K for $CO + H$ (Fuchs et al. 2009). If we assume first-order kinetics and a constant pre-exponential factor in both reactions, the effective barrier to reaction (2) is 384 ± 40 K, where the error is derived from the barrier to hydrogenation of CO. This is the first calculation of the effective barrier to reaction (2) in the solid phase, and our result is contradictory to that of Oba et al (2010), who conclude in their study that the reaction proceeds with little or no activation barrier but do not calculate a value. As suggested above, the presence of some fraction of excited OH in the beam could

produce CO_2 in a barrierless reaction with CO. Current grain models include grain surface activation barriers to reaction (2) of, e.g., 80 K (Y. Aikawa 2010, private communication) or 176 K (Cuppen et al. 2009), which would seem very low for an effective first-order rate equation, potentially overproducing CO_2 . All evidence suggests that $CO + OH$ is a more efficient route to CO_2 formation than the nonenergetic $CO + O$ route (reaction (1)), yet Roser et al. (2001) estimate that the barrier to reaction (1) is only 290 K and suggest that the reaction proceeds under quiescent cloud conditions. If this were correct, then in contrast to the results of Fuchs et al. (2009) and those presented here, $CO + O$ would be more likely to proceed than either $CO + H$ or $CO + OH$.

We feel, therefore, that it is relevant to briefly address the value of the $CO + O$ barrier as derived by Roser et al. (2001), which, if implemented in gas-grain models, would result in the incorrect pathway to CO_2 formation dominating the reaction scheme. Roser et al. (2001) derived the barrier from an experiment where a water ice cap was deposited on top of CO that had previously been exposed to O atoms, assuming that reaction (1) occurred in the water pores as the surface was heated, and explicitly relying upon the reagents being trapped at the surface by the water ice cap. Although other laboratory studies show that CO trapping can occur in water ice pores (Collings et al. 2003), observations and models confirm that CO freeze-out occurs after the formation of water ice layers in both molecular clouds (Pontoppidan et al. 2003) and protostellar disks (Visser et al. 2009), implying that a water ice cap is not a realistic mimic of any interstellar ice, including those found in quiescent regions. In fact, scenarios investigating reaction (1) by Roser et al. (2001) under conditions comparable to those present in quiescent molecular clouds yielded no CO_2 , nor did subsequent experimental studies by Oba et al. (2010). Together with the effective barrier to reaction (2) of 384 ± 40 K presented here, this suggests the importance of readdressing the value of the $CO + O$ barrier implemented in astrochemical models.

4. ASTROPHYSICAL IMPLICATIONS

The reaction of $CO + OH$ is seen to be viable under astrophysical conditions of temperature and pressure on silicate and np - H_2O surfaces. Small quantities of CO_2 were produced, in competition with other reactions involving OH (for example, the hydrogenation of OH to form H_2O). Thus, the mechanism $CO + OH$ could be key to explaining the formation of $CO_{2(s)}$ at the edges of dark clouds (low A_V), where $CO_{2(s)}$ is seen to form concurrently with H_2O on bare dust grains (Pontoppidan 2006), before a large quantity of CO ice becomes present.

By modeling the reaction we have determined the empirical relationship $k_{CO+H} \ll k_{CO+OH} < k_{H_2O_2+H} < k_{OH+H}, k_{O_2+H}$, where the overall effective rate of $CO + OH$ is determined to be 24 times slower than $OH + H$, and 1.7 times faster than $CO + H$, indicating why H_2O ice is always the most abundant species.

In dense molecular clouds, gas-phase hydrogen is observed to be mainly in the molecular form, but atomic H is present at a constant low abundance ($H/H_2 \sim 10^3$; Li & Goldsmith 2003) due to the balance of H_2 formation on grain surfaces and its destruction by cosmic rays. The abundance of OH increases with density, in line with that of O (see, e.g., Harju et al. 2000; Quan et al. 2008). Thus, after the freeze-out of CO, the reaction $CO + OH$ could proceed on the ice mantle due to higher abundances of CO on the grain surface. As the abundance of OH increases, so does the potential for formation of CO_2 via $CO + OH$. The formation of H_2O via the competitive reaction $OH + H$ will

also increase with density, and thus CO₂ and H₂O formation in central, more quiescent regions of molecular clouds is possible. This conclusion agrees well with the postulations of Goumans et al. (2008).

We are grateful to Marius Lewerenz and David Field for helpful discussions. J.A.N. thanks the Leverhulme Trust, the Scottish International Education Trust, the University of Strathclyde, and the Scottish Universities Physics Alliance for funding. The research leading to these results has received funding from the European Community's Seventh Framework Programme FP7/2007-2013 under grant agreement No. 238258. We acknowledge the support of the national PCMI programme founded by CNRS, the Conseil Régional d'Ile de France through SESAME programmes (contract I-07-597R), the Conseil Général du Val d'Oise, and the Agence Nationale de Recherche (contract ANR 07-BLAN-0129). We thank Jean-Louis Lemaire, Saoud Baouche, and Henda Chaabouni.

REFERENCES

- Alagia, M., Balucani, N., Casavecchia, P., Stranges, D., & Volpi, G. G. 1993, *J. Chem. Phys.*, **98**, 8341
- Amiaud, L., Dulieu, F., Fillion, J.-H., Momeni, A., & Lemaire, J. L. 2007, *J. Chem. Phys.*, **127**, 709
- Amiaud, L., Fillion, J. H., Baouche, S., Dulieu, F., Momeni, A., & Lemaire, J. L. 2006, *J. Chem. Phys.*, **124**, 094702
- Baulch, D. L., et al. 2005, *J. Phys. Chem. Ref. Data*, **34**, 757
- Bisschop, S. E., Fuchs, G. W., van Dishoeck, E. F., & Linnartz, H. 2007, *A&A*, **474**, 1061
- Chen, W. C., & Marcus, R. A. 2005, *J. Chem. Phys.*, **123**, 094307
- Collings, M. P., Dever, J. W., Fraser, H. J., McCoustra, M. R. S., & Williams, D. A. 2003, *ApJ*, **583**, 1058
- Cuppen, H. M., van Dishoeck, E. F., Herbst, E., & Tielens, A. G. G. M. 2009, *A&A*, **508**, 275
- de Graauw, T., et al. 1996, *A&A*, **315**, L345
- D'Hendecourt, L. B., & Jourdain de Muizon, M. 1989, *A&A*, **223**, L5
- Dulieu, F., Amiaud, L., Congiu, E., Fillion, J.-H., Matar, E., Momeni, A., Pirronello, V., & Lemaire, J. L. 2010, *A&A*, **512**, A30
- Ehrenfreund, P., Boogert, A. C. A., Gerakines, P. A., Tielens, A. G. G. M., & van Dishoeck, E. F. 1997, *A&A*, **328**, 649
- Frost, M. J., Sharkey, P., & Smith, I. W. M. 1993, *J. Chem. Phys.*, **97**, 12254
- Fuchs, G. W., Cuppen, H. M., Ioppolo, S., Romanzin, C., Bisschop, S. E., Andersson, S., van Dishoeck, E. F., & Linnartz, H. 2009, *A&A*, **505**, 629
- Fujii, T., Selvin, P. C., & Iwase, K. 2002, *Chem. Phys. Lett.*, **360**, 367
- Fulle, D., Hamann, H. F., Hippler, H., & Troe, J. 1996, *J. Chem. Phys.*, **105**, 983
- Gerakines, P. A., Schutte, W. A., & Ehrenfreund, P. 1996, *A&A*, **312**, 289
- Gerakines, P. A., et al. 1999, *ApJ*, **522**, 357
- Gibb, E. L., Whittet, D. C. B., Boogert, A. C. A., & Tielens, A. G. G. M. 2004, *ApJS*, **151**, 35
- Goumans, T. P. M., Uppal, M. A., & Brown, W. A. 2008, *MNRAS*, **384**, 1158
- Greenberg, J. M. 2002, *Surf. Sci.*, **500**, 793
- Harju, J., Winnberg, A., & Wouterloot, J. G. A. 2000, *A&A*, **353**, 1065
- Ioppolo, S., Cuppen, H. M., Romanzin, C., van Dishoeck, E. F., & Linnartz, H. 2008, *ApJ*, **686**, 1474
- Ioppolo, S., Cuppen, H. M., van Dishoeck, E. F., & Linnartz, H. 2011a, *MNRAS*, **410**, 1089
- Ioppolo, S., Palumbo, M. E., Baratta, G. A., & Mennella, V. 2009, *A&A*, **493**, 1017
- Ioppolo, S., van Boheemen, Y., Cuppen, H. M., van Dishoeck, E. F., & Linnartz, H. 2011b, *MNRAS*, **413**, 2281
- Jamieson, C. S., Mebel, A. M., & Kaiser, R. I. 2006, *ApJS*, **163**, 184
- Knez, C., et al. 2005, *ApJ*, **635**, L145
- Laffon, C., Lasne, J., Bournel, F., Schulte, K., Lacombe, S., & Parent, Ph. 2010, *Phys. Chem. Chem. Phys.*, **12**, 10865
- Lemaire, J. L., Vidali, G., Baouche, S., Chehrouri, M., Chaabouni, H., & Mokrane, H. 2010, *ApJ*, **725**, L156
- Lester, M. I., Pond, B. V., Anderson, D. T., Harding, L. B., & Wagner, A. F. 2000, *J. Chem. Phys.*, **113**, 9889
- Lester, M. I., Pond, B. V., Marshall, M. D., Anderson, D. T., Harding, L. B., & Wagner, A. F. 2001, *Faraday Discuss.*, **118**, 373
- Li, D., & Goldsmith, P. F. 2003, *ApJ*, **585**, 823
- McKinley, J. D., Garvin, D., & Boudart, M. J. 1955, *J. Chem. Phys.*, **23**, 784
- Médard, N., Soutif, J.-C., & Poncin-Epaillard, F. 2002, *Langmuir*, **18**, 2246
- Mennella, V., Baratta, G. A., Palumbo, M. E., & Bergin, E. A. 2006, *ApJ*, **643**, 923
- Mennella, V., Palumbo, M. E., & Baratta, G. A. 2004, *ApJ*, **615**, 1073
- Miyauchi, N., Hidaka, H., Chigai, T., Nagaoka, A., Watanabe, N., & Kouchi, A. 2008, *Chem. Phys. Lett.*, **456**, 27
- Mokrane, H., Chaabouni, H., Accolla, M., Congiu, E., Dulieu, F., Chehrouri, M., & Lemaire, J. L. 2009, *ApJ*, **705**, L195
- Nummelin, A., Whittet, D. C. B., Gibb, E. L., Gerakines, P. A., & Chiar, J. E. 2001, *ApJ*, **558**, 185
- Oba, Y., Watanabe, N., Kouchi, A., Hama, T., & Pirronello, V. 2010, *ApJ*, **712**, L174
- Oliveira, J. M., et al. 2011, *MNRAS*, **411**, L36
- Palumbo, M. E., Baratta, G. A., Brucato, J. R., Castorina, A. C., Satorre, M. A., & Strazzulla, G. 1998, *A&A*, **334**, 247
- Pontoppidan, K. M. 2006, *A&A*, **453**, L47
- Pontoppidan, K. M., et al. 2003, *A&A*, **408**, 981
- Pontoppidan, K. M., et al. 2008, *ApJ*, **678**, 1005
- Quan, D., Herbst, E., Millar, T. J., Hassel, G. E., Lin, S. Y., Guo, H., Honvault, P., & Xie, D. 2008, *ApJ*, **681**, 1318
- Roser, J. E., Vidali, G., Manicò, G., & Pirronello, V. 2001, *ApJ*, **555**, L61
- Ruffle, D. P., & Herbst, E. 2001, *MNRAS*, **324**, 1054
- Shimonishi, T., Onaka, T., Kato, D., Sakon, I., Ita, Y., Kawamura, A., & Kaneda, H. 2010, *A&A*, **514**, A12
- Smith, I. W. M., & Zellner, R. 1973, *J. Chem. Soc. Faraday Trans. II*, **69**, 1617
- Sun, H., & Law, C. K. 2008, *THEOCHEM*, **862**, 138
- Talbi, D., Chandler, G. S., & Rohl, A. L. 2006, *Chem. Phys.*, **320**, 214
- van Dishoeck, E. F., et al. 1996, *A&A*, **315**, L349
- Visser, R., van Dishoeck, E. F., Doty, S. D., & Dullemond, C. P. 2009, *A&A*, **495**, 881
- Watanabe, N., & Kouchi, A. 2002, *ApJ*, **571**, L173
- Whittet, D. C. B., et al. 1998, *ApJ*, **498**, L159
- Williams, D., & Herbst, E. 2002, *Surf. Sci.*, **500**, 823
- Yu, H. G., Muckerman, J. T., & Sears, T. J. 2001, *Chem. Phys. Lett.*, **349**, 547